PROFILE STUDIES OF ION-IMPLANTED MESFETs*

J. M. Golio and R. J. Trew

Electrical Engineering Dept.
North Carolina State University
Raleigh, North Carolina 27650

ABSTRACT

A study of ion-implanted MESFET performance as a function of the implantation energy and fluency and including the effects of deep-level trap concentrations in the substrate has been conducted. Carrier concentrations as a function of depth are determined through the use of LSS theory and a profiling model. An analytic device model, which computes both DC and RF characteristics, is then employed to predict MESFET performances. The study includes the effects of depth dependent transport properties and has indicated a number of design rules for the fabrication of optimized ion-implanted devices.

INTRODUCTION

The performance of FETs fabricated by ion-implantation depends greatly on carrier concentrations and velocity-field characteristics as a function of depth into the active device layers. The presence of deep-level traps in the semiconductor contributes to the complexity of problems associated with the characterization of ion-implanted devices.

This work is targeted mainly at determining design rules for high-frequency ion-implanted MESFETs. The study utilizes theoretical models of both material properties and device characteristics. This information is combined with experimental material characterization to provide improved quantitative accuracy of the model.

Initially, the determination of typical ranges for concentrations of deep-level traps, $N_T(x)$ (normally due to chromium in the GaAs substrate) was made from a novel measurement technique using both differential capacitance and conductance DLTS data. Shallow-level donor concentrations, $N_D(x)$, were then determined from LSS theory as a function of implantation parameters. These concentrations as a function of depth were then used in a profiling model to determine the free-carrier profile, n(x), for the material. Carrier transport properties were also determined from the trap and donor profiles. This was done through the use of Monte Carlo particle simulations and a model to account for the effects of compensation in the semiconductor.

An analytic model which utilizes all of this information is then used to assess performance potential. The distinction between free-carrier and donor profiles, the effect of deep-level traps, and the depth dependance of mobility and velocity are shown to be important considerations which have been ignored in previous models. The DC characteristics and small-signal S-parameters along with figures of merit are computed by the model.

MATERIAL CHARACTERIZATION

Figure 1 shows free-carrier, background donor, and deep-level trap profiles typical of ion-implanted semiconductor material. Deep-level trap centers and free-carrier diffusion from highly doped to lowly doped regions will cause the free-carrier profile to differ from that of the ionized donors. Our studies show that as much as an order of magnitude difference can exist between these two profiles for ion-implanted materials typically used in the fabrication of GaAs MESFETs. The deep-level sites will also have a degrading effect on carrier transport properties.

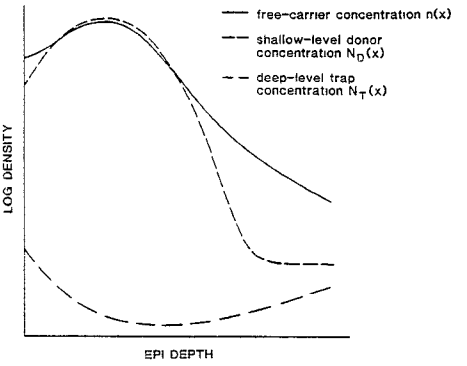

Figure 1 Typical concentraion profiles for ion-implanted material.

Determination of the various profiles present in a sample is a difficult problem. Traditional C-V analysis measures the free-carrier concentration if traps are not present [1]. When traps are present, however, knowledge of the trap concentration profile is neccessary to extract the free-carrier information [2]. Likewise, DLTS data can give trap concentration information if the free-carrier profile is known. For this work,

---

*This work was supported by Rockwell International Electronics Research Center and the U. S. Army Research Office, Research Triangle Park, NC on contract DAAG29-80-K-0080.

these two methods were combined to determine the free-carrier, shallow-level donor and deep-level trap concentrations for a typical ion-implanted device. The details of this technique are discussed elsewhere [3]. Needed for the technique is the low-field mobility of the material as a function of donor density and background compensation. This is obtained using the theoretical results of Walukiewicz et al. [4] in conjunction with Monte Carlo velocity-field predictions. Our own Monte Carlo results [5] were used to determine the mobility as a function of background donor density with no traps present, and the Walukiewicz values were then normalized to the Monte Carlo numbers. The normalized data was finally curve fit to obtain an empirical expression for mobility as a function of background donor density and compensation ratio. The resulting expression is

$$\mu_o = \frac{\mu_{max}}{1 + \left(\frac{\log N_D}{N_o}\right)^c} \cdot (1-\theta)^b \qquad (1)$$

where

μ_{max} = 8380 ($cm^2/v*sec$),
N_o = 23.2553,
c = 23.0,
$\theta = N_T/N_D$,
$b = A(\log N_D)^2 - B(\log N_D) + C$ for $N_D > 10^{21}$ (m^{-3}),
$b = 0.114992$ for $N_D < 10^{21}$ (m^{-3}),

with

A = 0.025,
B = 0.817278,
C = 6.252838

and where N_D is given in (m-3). Expression (1) is plotted against the normalized Walukiewicz values

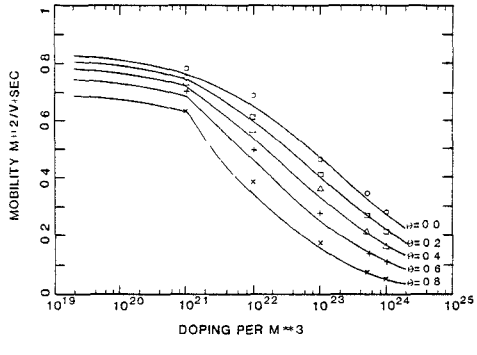

Figure 2 Low-field mobility as a function of doping and deep-level compensation. The solid lines are computed from equation (1) for θ=0.0, 0.2, 0.4, 0.6, 0.8. The data points are from the normalized theoretical computations [4].

in Figure 2. As can be seen from the plot, the agreement is quite good.

A one micron gate length MESFET along with a differential capacitance pattern were fabricated on Silicon implanted Cr-doped GaAs substrate. Conductance DLTS and C-V measurements were performed on these devices and a dominant deep-level trap state was identified 0.736 eV below the conduction band. The measurements were used as input data to a computer simulation which computes the desired profiles as mentioned above.

The final resulting free-carrier, shallow-level donor, and deep-level trap concentrations as a function of depth into the material are shown in

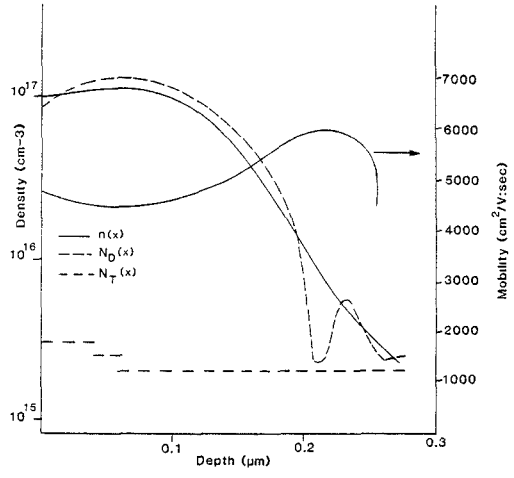

Figure 3 Resulting concentration profiles and low-field mobility profile for one device.

Figure 3. Notice that deep into the channel there is some scatter of the shallow-level donor data. This begins to occur when the trap concentration and the shallow-level donor concentration are of the same order of magnitude. The uncertainties in the exact shallow-level concentration at this depth into the channel are not critical to the profile predictions. This is true since the magnitude of all the profiles of interest are small at this depth when compared to their magnitudes near the implantation peak.

The low-field mobility profile obtained from this analysis is also shown in Figure 3. The curve can be compared to the results of Das and Kim [6], and is in good qualitative agreement.

THE DEVICE MODEL

The device model used here is a one-dimensional model with a small-signal analysis. One-dimensional models offer a number of advantages for a study of this type over more elaborate two-dimensional models. For example, the form of the results obtained from one-dimensional analysis is more useful in terms of many device optimization and design problems. Also, information needed to examine circuit/device interface phenomena can easily be obtained from one-dimensional results. Of critical importance here, however, is the cost difference between one- and two-dimensional simulations. In these studies, over one-hundred different device geometries were examined at ten to twenty different bias levels. To obtain this

information from two-dimensional simulations would have been at least an order of magnitude more costly in terms of both time and money.

The model assumes that the electron transport properties of a material can be simulated by a two-piece velocity-field relationship. The two-piece approximation is defined from a theoretical velocity-field characteristic determined by Monte Carlo techniques. For electric fields less than an appropriate saturation field, E_m, the electron velocity is described by a linear expression,

$$v = \mu_o E. \tag{2}$$

For electric fields above E_m the electrons move at a constant, maximum velocity, v_m. Using this information, a small-signal equivalent circuit as shown in Figure 4 can be determined and analyzed to obtain RF performance predictions, including power gains as a function of frequency.

Low-field mobility as a function of depth for the model is obtained directly from equation (1). Determining the appropriate maximum velocity for the material is more involved, however.

The importance of developing a systematic, well-justified technique for determining maximum velocity, v_m, was discussed in earlier work [7,8] and in this study, such a method has been developed. The method involves numerical determination of the carrier transit time under the gate using an exact velocity-field relationship. The assumed field distribution for this calculation is obtained from two-dimensional simulation results. It is then required that the transit time calculated assuming a two-piece approximated velocity-field relationship be equal to that of the exact analysis. This method yields a v_m for GaAs (doped to a level $N_D = 10^{17}cm^{-3}$) in excellent agreement with the value obtained by Pucel et al. [9]. The resulting data was curve fit and expressed as

$$v_m = v_o - A \log [(1-y)^2 + By] \tag{3}$$

where

$y = (N_D(x)/N_o)^{2.5}$,
$N_o = 1.5 \times 10^{22}$,
$A = 0.0262$,
$B = 0.4$,
$v_o = 1.40$.

Equation (3) gives v_m in 10^5 m/sec when $N_D(x)$ is expressed in m^{-3}. The expression is also assumed to have the same dependence on compensation ratio, θ, as equation (1). Thus, the factor $(1 - \theta)^b$ is multiplied with equation (3) to obtain v_m in the presence of traps. The exponent, b, is defined in equation (1).

Equations (1) and (3) in conjunction with knowledge of the three profiles, n(x), $N_D(x)$ and $N_T(x)$, allow for the derivation of a device model which includes the effects of varying transport properties as a function of epi-depth.

The current-voltage predictions of the model for a one micron ion-implanted device are compared

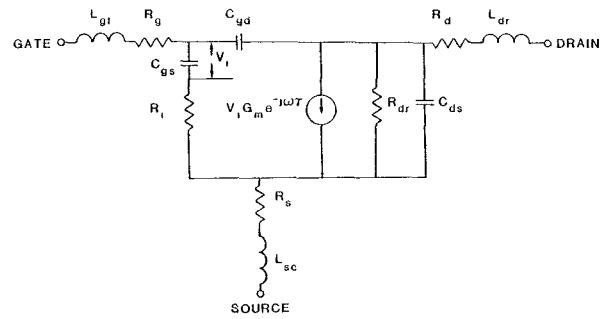

Figure 4 The equivalent circuit for an FET used in the analysis.

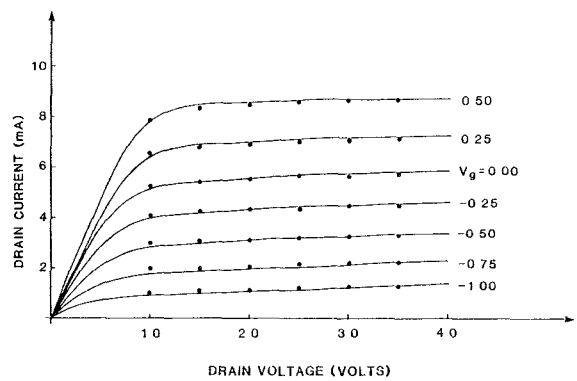

Figure 5 Comparison of model predicted and measured I-V characteristics for a one micron ion-implanted device.

in Figure 5 with the measured I-V curves. The agreement is excellent. It should be noted that without the inclusion of the effects of traps on carrier transport, this agreement could not be obtained. The traps have a tendency to "soften" the pinch-off characteristics of the device (ie. when traps are included in the simulation, the slope dI_D/dV_g is not as great near pinch-off). For all of the devices studied in this work, this "softening" effect was required to obtain best agreement with measured I-V characteristics.

RESULTS AND CONCLUSIONS

The results that follow were obtained following the modeling steps outlined in the Introduction. Three parameters were varied independently. They are 1) implantation energy, ξ, 2) peak doping density, N_{max}, and 3) trap concentration, $N_T(x)$. The implant species was assumed to be Si in GaAs and the activation was assumed to be 100% for all devices. The trap concentration was assumed to be constant as a function of depth for these studies. Note that the peak doping density can be converted to a corresponding ion fluency through the simple relationship

$$\phi = \sqrt{2\pi}\, \sigma_p\, N_{max} \tag{6}$$

where σ_p is the standard deviation of the

projected range.

For the implant energy and peak doping studies, the trap level was left constant at $N_T=2.0 \times 10^{15}$ cm^{-3}. This number was chosen to be in general agreement with the results shown in Figure 3. The implant energy was varied from 50 to 150 keV while the peak doping took values between 8×10^{16} and 4×10^{17} cm^{-3}.

Figures 6a and 6b illustrate the effects these parameters have on the gain-bandwidth product, f_T,

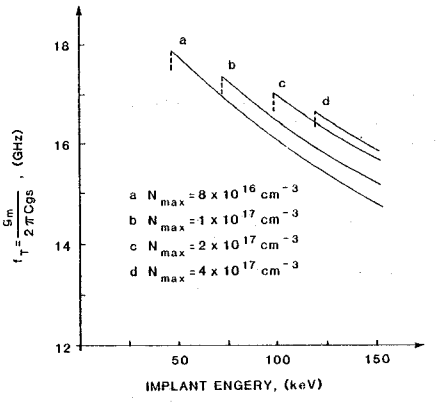

Figure 6a Predicted gain-bandwidth product, f_T, vs. implantation energy, $\mathcal{E}$. The peak doping, N_{max}, is used as an independent parameter.

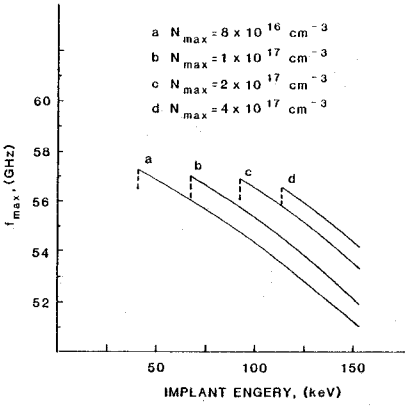

Figure 6b Predicted maximum frequency of oscillation, f_{max}, vs. implantation energy, $\mathcal{E}$. The peak doping, N_{max}, is used as an independent parameter.

and the maximum frequency of oscillation, f_{max}. The value for f_T is computed from first order considerations to be given by

$$f_T = g_m/2\pi C_{gs}. \qquad (7)$$

The quantity f_{max} is obtained by noting the frequency at which Mason's unilateral gain (as predicted by the model) goes to unity. The results clearly indicate the superiority of low-energy implants for high-frequency operation.

All of the devices considered in compiling Figures 6a and 6b were compared at a bias of I_D=10 mA. The dashed line falling off rapidly at the low-energy end of the curves indicates that for energies lower than this, I_{DSS}<10 mA.

For the trap study, an implant energy of 70 keV and a peak doping density of 2×10^{17} cm^{-3} was assumed. The background trap concentration was varied from 0 to 10^{16} cm^{-3}.

Figure 7 illustrates the effects traps have on the zero gate bias current, I_{DSS}, and the pinch-off potential, W_{OO}. Figure 8 shows the pinch-off "softening" effect mentioned in the previous

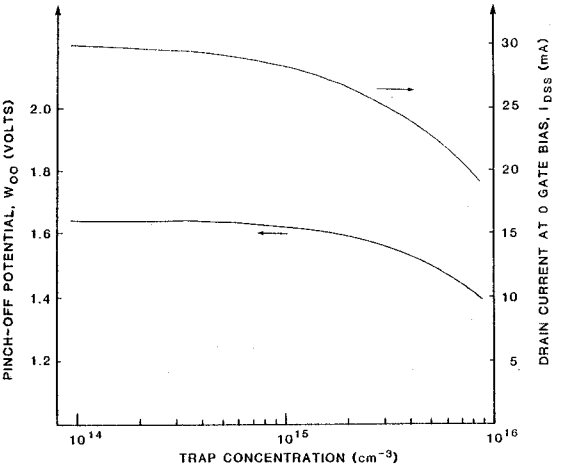

Figure 7 Predicted effects of varying trap concentrations on DC characteristics.

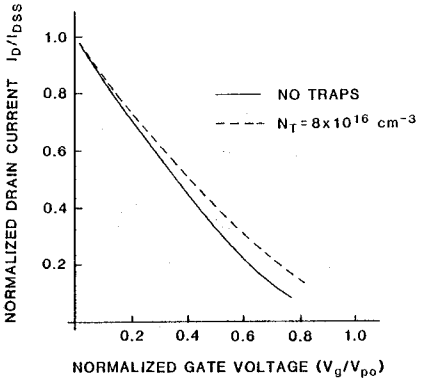

Figure 8 Normalized drain current predictions vs. normalized gate voltage with and without traps.

section for one particular device.

Deep-level traps also have some effect on the RF performance of the device as illustrated in Figures 9 and 10. Figure 9 shows clearly the decrease of f_T and f_{max} associated with increasing trap concentrations.

In Figure 10 note that for low bias currents f_T increases when few traps are present while it decreases for higher trap concentrations. This is easily explained in terms of the degrading effects traps have on mobility and velocity. As the gate bias restricts current flow, a larger fraction of the carriers are forced deeper into the channel.

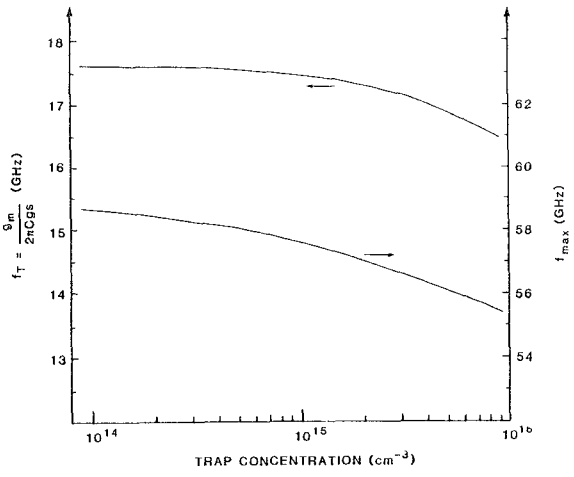

Figure 9 Predicted gain-bandwidth product, f_T, and maximum frequency of oscillation, f_{max}, vs. background trap concentration.

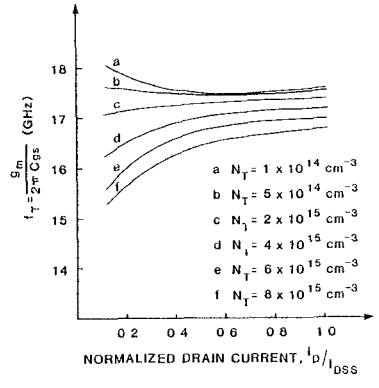

Figure 10 Predicted gain-bandwidth product, f_T, as a function of normalized drain current. The background trap concentration is used as a variable parameter.

This corresponds to the more lightly doped regions of the device. If the compensation ratio is fairly small (ie. few traps) then from equations (1) and (3) the transport properties are superior, and f_T increases. If, on the other hand, the trap level is on the same order of magnitude as the shallow-level donor concentration, then the compensation ratio approaches one. This corresponds to extreme degradation of mobility and velocity and, thus, forces f_T to decrease.

In conclusion, deep level traps in ion-implanted devices degrade carrier transport properties in the semiconductor material. The degradation is more severe near the tail of the implant profile than near the peak. Thus, the transport properties of the device will be depth -- or bias -- dependent. A modeling technique which accounts for this dependence has been used to study device properties as a function of fabrication parameters and deep-level trap concentrations. The results indicate that low energy implants should posess superior high-frequency properties and that lowering the trap levels in the material should improve device performance.

REFERENCES

1. D. P. Kennedy, R. R. O'Brien,"On The Measurement of Impurity Atom Distributions by the Differential Capacitance Technique," IBM Journal of Research and Development, pp. 212-214, March 1969.

2. L. C. Kimerling,"Influence of Deep Traps on the Measurements of Free-Carrier Distributions in Semiconductors by Junction Capacitance Techniques," Journal of Applied Physics, vol. 45, pp. 1839-1845, April 1974.

3. J. M. Golio, R. J. Trew and H. Lefever, "A Characterization Technique For Ion-Implanted GaAs MESFETs," submitted for publication.

4. W. Walukiewicz, L. Lagoaski, L. Jastrzebski, M. Lichtensteiger, and H. C. Gatos, "Electron Mobility and Free-carrier absorption in GaAs: Determination of the compensation ratio," Journal of Applied Physics, vol. 50, pp. 899-908, Feb. 1979.

5. M. A. Littlejohn, J. R. Hauser, T. H. Glisson,"Velocity-field Characteristics of GaAs with Γ_6^C -L_6^C-X_6^C Conduction-band Ordering," Journal of Applied Physics, vol. 48, pp. 4587-4590, Nov. 1977.

6. M. B. Das, B. Kim,"Mobility and Carrier Concentration Profiles in Ion-Implanted Layers on Doped and Undoped Semi-Insulating GaAs Substrates at 299 and 105 K," IEEE Transactions on Electron Devices, vol. ed-29, pp.205-211, Feb. 1982.

7. J. M. Golio, "Compound Semiconductors for Microwave MESFET Applications," Masters of Science Thesis, North Carolina State University, Raleigh, North Carolina, May 1980.

8. J. M. Golio and R. J. Trew, "Compound Semiconductors for Low-Noise Microwave MESFET Applications," IEEE Trans. Electron Devices, vol. ED-27, July 1980, pp. 1256-1262.

9. R. A. Pucel, H. Statz, H. A. Haus, "Signal and Noise Properties of Gallium Arsenide Microwave Field-Effect Transistors," Advances in Electronics and Electron Physics. New York: Academic, vol. 38, pp. 195-265, 1975.